# Numerical Methods in Analyzing White Dwarf Structure

Ayush Roy

July 2021

**Abstract**

White dwarfs, neutron stars and black holes are the three currently known final fates of stars. The end result of a star is highly dependent on the mass of its core, and star's with relatively lower core masses (popular fiducial mass value is lower than 10 solar masses) end up as white dwarfs. These are supported against gravitational collapse by electron degeneracy pressure which is a result of a sea of electrons created by complete ionization of carbon, nitrogen and oxygen obeying quantum-mechanical statistics, as discussed in Section 1. The goal of this paper is to use theoretical principles to numerically solve for the mass, radius and density of white dwarfs, and the standard skeleton of stellar structure code is provided in Section 2. The ingredient required by this algorithm is the equation of state, which is developed in Section 3, most of which is based on the works of reference [1]. To test correctness of the derived result, results are compared with the poly-tropic equation of state in the extreme non-relativistic and relativistic limits in Section 4. Section 5 scales the fundamental constants of the problem to those suitable for computation, and Section 6 displays results for the mass-radius relationship, mass profile and density profile for carbon and iron white dwarfs. Section 7 provides an alternate approach to this problem using de-coupling of first order differential equations to one single second-order differential equation. The derived result is coined as the Roy-Lane-Emden Equation. Section 8 summarizes this discussion, and Section 9 mentions some further computational problems for white dwarfs.

## 1 Theoretical Background

White dwarfs are one of the three currently known final fates of stars. Stars begin their life as proto-stars, drawing gas from the proto-planetary disk. Hydrogen burning begins when the temperature of their cores overcomes the Coulomb Barrier for two protons, paving the way for helium and energy production by the **proton-proton chain**. This is the **Main Sequence Phase** of the star's life and is the longest phase of energy production.

Hydrogen burning begins at the core and proceeds outwards, increasing the temperature and pressure of the envelope causing the radius and luminosity to increase. Hydrogen is exhausted first in the core, and once the temperature is favourable, helium is fused to carbon by the **triple-alpha process**. The beginning of this violent and relatively quick burning phase is signalled by the **helium flash**.

Depending on the star's core mass, temperatures may be high enough to induce carbon burning all the way to the top of the nuclear binding curve and produce an iron core which can no longer provide pressure support against gravity. Such massive stars blow away their envelopes in a violent **supernova** and the core collapses under the action of gravity. Moderately massive stars are supported by neutron **degeneracy pressure**, and are fittingly called **neutron stars**. Extremely massive stars which can't be supported by degeneracy pressure under collapse end up as **black holes**.

The focus of this paper is on those lighter star's which don't reach temperatures sufficient enough to induce carbon burning, and the core collapses earlier than their more massive counterparts. After such stars shed their envelope as **planetary nebulae**, core collapse scenario is halted by **electron degeneracy pressure** and the eventual state of the star is a **white dwarf**. White dwarfs are dim and relatively light stellar graveyards rich in carbon, nitrogen and oxygen. It may be possible for the core to get hot enough while the star is in the white dwarf phase so that these elements burn up to iron, making a supernova a possibility. Much like the helium flash, the onset of carbon burning is marked by the **carbon flash**.

The temperature in a white dwarf's core is high enough to completely ionize carbon, nitrogen and oxygen. ALso, at high densities and for white dwarf temperatures at which ($k_B T << E$), the quantum mechanical **Fermi-Dirac Distribution** forces these free electrons arising from ionization to fill all energy states up till a maximum energy value, called the **Fermi Energy**. Moreover, the **Pauli Exclusion Principle** allows two electrons in each state, which coupled with the Fermi-Dirac Distribution creates a dense electron environment that can support the white dwarf against gravitational collapse. This pressure support is electron degeneracy pressure, and is key in modelling white dwarf stars.

The goal of this paper is to utilize known and tested physical laws and numerically solve for the mass, density and radius of a white dwarf subject to composition and density. At low densities, white dwarf electrons are

non-relativistic and theory predicts an inverse cubic relationship between mass and radius. At extremely high densities, electrons of the white dwarf are relativistic and the mass approaches the **Chandrasekhar Limit**, equal to 1.44 solar masses for carbon white dwarfs, along with a rapidly shrinking radius. These attributes are tested for using numerical methods.

# 2 Stellar Structure Algorithm: First Order Diff Eq

The general mechanism of stellar structure problems is to numerically solve two coupled first-order differential equations. The first of them comes from mass conservation:

$$\frac{dm}{dr} = \rho(r)d\Omega = \rho(r)\int_0^{2\pi} d\phi \int_0^{\pi} sin\theta d\theta = 4\pi r^2 \rho(r), \tag{1}$$

and the second is a result of hydro-static equilibrium and some algebra as follows:

$$\frac{dP}{dr} = \frac{dP}{d\rho}\frac{d\rho}{dr} \implies \frac{d\rho}{dr} = \frac{dP}{dr}\left(\frac{dP}{d\rho}\right)^{-1} = -\left(\frac{dP}{d\rho}\right)^{-1}\frac{Gm(r)\rho(r)}{r^2}. \tag{2}$$

The further key ingredient needed is the quantity $\frac{dP}{d\rho}$ present in (2). This would be obtainable if we had $P(\rho)$, and is the **equation of state** for the star being probed. Once this is obtained, (1) and (2) are solved using the Euler algorithm given explicitly by:

$$m[i+1] = m[i] + 4\pi r^2[i]\rho[i]dr, \tag{3}$$

$$\rho[i+1] = \rho[i] - \left(\frac{dP}{d\rho}\right)^{-1}_{m[i],r[i],\rho[i]} \frac{Gm[i]\rho[i]}{r^2[i]}dr. \tag{4}$$

Normally for such exercises, the method begins by imposing an initial doublet ($\rho[r=0] = \rho_c, m[r=0] = 0$) where $\rho_c$ is the central density, but there is a discontinuity at $r = 0$ for (4) so the same values for the density and mass are imposed at $r = dr$. Changing values for the central density changes results of the routine.

A qualitative examination of (3) and (4) tells that the mass will increase as integration goes outwards with the rate of increase linearly proportional to the density. For all realistic equation of states, the density will decrease through constant outward integration, with the rate of decrease steep at first for smaller values of $r$ and then a gradual levelling to zero. For this exercise, **the radius of the star is set by when the density first drops to zero or below zero**. The mass at this radius value then marks the total mass of the star.

# 3 Deriving the Equation of State

## 3.1 Deriving Energy and Critical Density

To find the equation of state $P(\rho)$, the white dwarf is essentially treated as a **sea of degenerate electrons that follow the Dirac distribution for fermions**. In this degenerate limit, there are essentially two electrons per energy state and the value for the highest wave vector (wave vector is related to momentum by the De-Broglie relation $p = \hbar k$), called the Fermi wave vector is given by

$$k_f = \left(3\pi^2 n\right)^{\frac{1}{3}}, \tag{5}$$

where $n = \frac{N}{V}$ is the number density of matter. The energy of the white dwarf is given by averaging the energy of electrons over all values of the wave vector up to the Fermi wave vector given in (5). The result is derived in reference [1] and is quoted in (6):

$$E = Vn_0 m_e c^2 x^3 \epsilon(x), \quad x = \frac{p_f}{m_e c} = \left(\frac{n}{n_0}\right)^{\frac{1}{3}} = \left(\frac{\rho}{\rho_0}\right)^{\frac{1}{3}}, \tag{6}$$

where $x$ is the ratio of fermi momentum and the mass of the ecltron times the speed of light and $\epsilon(x)$ is a complicated function of this ratio which comes about after integration to find $E$. The last equality is especially important and introduces a **critical density which marks the transition from a non-relativistic electron sitting at the Fermi energy to a relativistic one**. This is easy to see in the following calculation:

$$p_f = \hbar\left(3\pi^2 n_0\right)^{\frac{1}{3}} = m_e c \implies n_0 = \frac{m_e^3 c^3}{\hbar^3 3\pi^2} = 5.89 \times 10^{29} cm^{-3}. \tag{7}$$

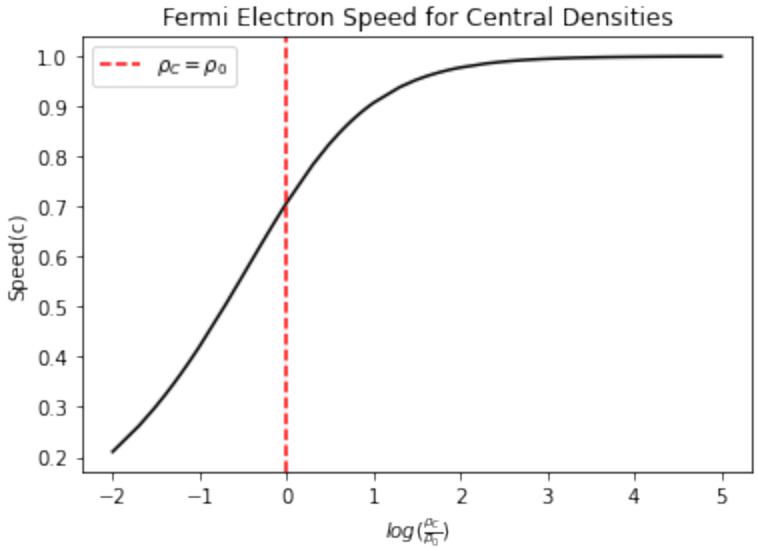


Figure 1: Fermi Electron Speed for Varying Central Density: This plot was made using (8), and shows how relativistic a fermi electron is when the central density of the white dwarf star is varied. The dashed line is the critical density and marks the transition from non-relativistic to relativistic regime. A fermi electron at this density has a momentum equal to rest mass multiplied by the speed of light.

A white dwarf star with a number density below $n_0$ can be treated as non-relativistic, where as those with higher values of number density than $n_0$ are treated relativistic. It is of intuitive interest to convert this notion into speeds, and Figure 1 plots the speed of an electron sitting in the Fermi wave vector state against the number density. Suppose $n = \kappa n_0$, the speed for a fermi electron becomes

$$\frac{\gamma m_e v}{\gamma m_e c^2} = \frac{p}{E} = \frac{p}{\sqrt{p^2c^2 + m_e^2 c^4}} \implies \frac{v}{c} = \frac{\kappa^{\frac{1}{3}}}{\sqrt{1+\kappa^{\frac{2}{3}}}}. \tag{8}$$

In the next few sections, it will be desirable to express this critical number density in terms of a mass density using

$$n_0 = \frac{\rho_0}{\mu m_H} \implies \rho_0 = \frac{n_0 m_H}{\chi_e}, \tag{9}$$

where $\mu$ strictly speaking is the average atomic mass in terms of amu whose inverse is $\chi_e$, the number of electrons per nucleon. This is justified because 1) elements in a white dwarf (C,N,O,Fe) are considered to be completely ionized meaning that electron count dominates nuclei count 2) the mass of an electron is negligible to the mass of a nucleon. $\chi_e$ calculations for carbon and iron are given below:

$$\frac{1}{\mu_C} = \frac{6+1}{12+\frac{6}{1000}} \approx \frac{6}{12} = 0.5 = \chi_{e,C}, \quad \frac{1}{\mu_{Fe}} = \frac{26+1}{56+\frac{26}{1000}} \approx \frac{26}{56} = 0.464 = \chi_{e,Fe}. \tag{10}$$

### 3.2 Thermodynamic Connections and Chain Rule

Continuing on with the goal of finding the equation of state, the first law of thermodynamics is invoked,

$$dE(V,S) = -PdV + TdS \implies P = -\frac{\partial E}{\partial V} = -\frac{\partial E}{\partial x}\frac{\partial x}{\partial V}, \tag{11}$$

and since by (6) energy is given as a function of density, (11) gives a way of finding $P(\rho)$, the desired relation. All one needs to do is to apply the chain rule and calculate a few derivatives as follows:

$$\frac{\partial E}{\partial x} = \frac{\partial}{\partial x}\left(V n_0 m_e c^2 x^3 \epsilon(x)\right) = \frac{\partial}{\partial x}\left(N m_e c^2 \epsilon(x)\right) = V n_0 m_e c^2 x^3 \epsilon^{'}(x), \tag{12}$$

$$\frac{\partial x}{\partial V} = \frac{\partial}{\partial V}\left(\frac{n}{n_0}\right)^{\frac{1}{3}} = \left(\frac{N}{n_0}\right)^{\frac{1}{3}} \frac{\partial (V^{\frac{-1}{3}})}{\partial V} = -\frac{x}{3V}, \tag{13}$$

and putting the results of (12) and (13) into (11), the equation of state is obtained as below:

$$P = \frac{1}{3} n_0 m_e c^2 x^4 \epsilon^{'}(x). \tag{14}$$

What goes into the stellar structure algorithm is the derivative of pressure with respect to density, so one more chain rule calculation is performed as below:

$$\frac{dP}{dx} = \frac{1}{3} n_0 m_e c^2 \frac{d}{dx}\left(x^4 \epsilon^{'}(x)\right), \tag{15}$$

$$\frac{dx}{d\rho} = \frac{1}{3\rho_0^{\frac{1}{3}}\rho^{\frac{2}{3}}} = \frac{1}{3\rho_0}\left(\frac{\rho_0}{\rho}\right)^{\frac{2}{3}} = \frac{1}{3x^2\rho_0}, \tag{16}$$

$$\frac{dP}{d\rho} = \frac{dP}{dx}\frac{dx}{d\rho} = \frac{1}{9x^2}\frac{\chi_e m_e c^2}{m_H}\frac{d}{dx}\left(x^4\epsilon^{'}(x)\right) = \alpha(x)\frac{\chi_e m_e c^2}{m_H}, \tag{17}$$

and I have invoked (9) in the last equality and $\alpha(x)$ is defined as:

$$\alpha(x) = \frac{1}{9x^2}\frac{d}{dx}\left(x^4\epsilon^{'}(x)\right) = \frac{x^2}{3\left(1+x^2\right)^{\frac{1}{2}}}, \tag{18}$$

with a respectful and compact form! This gives everything needed to begin with the stellar structure algorithm; the updated form of (2) is given below:

$$\frac{d\rho}{dr} = -\left(\frac{\chi_e m_e c^2 \alpha(x)}{m_H}\right)^{-1}\frac{Gm(r)\rho(r)}{r^2}. \tag{19}$$

# 4 Comparisons with the Poly-tropic Equation of State

It is worthwhile to check the correctness of the equation of state derived in (17) by considering extreme limits. The key quantity which changes is $\alpha(x)$, where $x = \frac{\rho}{\rho_0}$ is a measure of density in terms of critical density. In the non-relativistic limit,

$$\alpha(x)_{x<<1} \approx \frac{x^2\left(1-\frac{x^2}{2}\right)}{3} \approx \frac{x^2}{3} = \frac{1}{3}\left(\frac{\rho}{\rho_0}\right)^{\frac{2}{3}}, \tag{20}$$

so with this approximation (17) becomes

$$\frac{dP}{d\rho} = \left(\frac{\rho}{\rho_0}\right)^{\frac{2}{3}}\frac{\chi_e m_e c^2}{3m_H} \implies P = \frac{\chi_e m_e c^2}{\rho_o^{\frac{2}{3}} 5m_H}\rho^{\frac{5}{3}} = \frac{m_e^4 c^5}{5\hbar^3 3\pi^2}\left(\frac{\rho}{\rho_0}\right)^{\frac{5}{3}}, \tag{21}$$

where in the last equality I have invoked (9) and (7). In the relativistic limit, the $\alpha(x)$ parameter becomes:

$$\alpha(x)_{x>>1} \approx \frac{x}{3} \approx \frac{1}{3}\left(\frac{\rho}{\rho_0}\right)^{\frac{1}{3}}, \tag{22}$$

and with this approximation (17) becomes

$$\frac{dP}{d\rho} = \left(\frac{\rho}{\rho_0}\right)^{\frac{1}{3}}\frac{\chi_e m_e c^2}{3m_H} \implies P = \frac{\chi_e m_e c^2}{\rho_o^{\frac{1}{3}} 4m_H}\rho^{\frac{4}{3}} = \frac{m_e^4 c^5}{4\hbar^3 3\pi^2}\left(\frac{\rho}{\rho_0}\right)^{\frac{4}{3}}. \tag{23}$$

Observation of (21) and (23) tells that the equation of state in such extreme limits is given by a power law, which is the **poly-tropic equation of state** given by:

$$P = P_0\left(\frac{\rho}{\rho_0}\right)^{\Gamma}, \tag{24}$$

where $\Gamma$ is the **adiabatic index** and is equal to $\frac{5}{3}$ in the non-relativistic case and $\frac{4}{3}$ in the relativistic limit. Comparisons with (24) tells that the constant $P_0$ increases by a factor of $\frac{5}{4}$ from the non-relativistic to the relativistic limit. If one wants to simply model a white dwarf in these extreme limits, the poly-tropic equation of state can be used if supplied with a suitable $(\Gamma, \rho_C)$ combination, but for the general case the equation of state developed in Section 3 must be utilized.

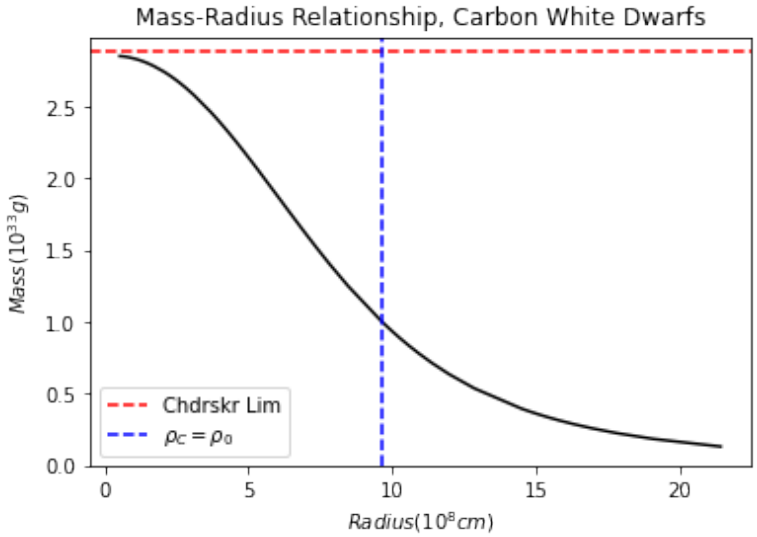


Figure 2: Mass-Radius Relationship for Carbon White Dwarfs: Solutions to the stellar structure code yields the mass-radius relationship for white dwarfs, subject to a value of $\chi_e$ and $\rho_C$. For carbon, $\chi_e = 0.5$. The dashed vertical line demarcates non-relativistic and relativistic limits. It is seen that non-relativistic white dwarfs are less massive and larger where as relativistic white dwarfs approach a mass value, the Chandrasekhar Limit, with a rapidly shrinking radius.

# 5 Units and Scaling

With learned insight, the most sensible units for modelling white dwarf mass and radius are solar masses and Earth radii respectively. Neglecting the leading constants for these values, the fundamental constants and the critical density implicitly buried in $\alpha(x)$ which appear in (19) transform as:

$$G = 6.67 \times 10^{-8} \left(\frac{cm^3}{gs^2}\right) \times \left(\frac{1R_e}{10^8 cm}\right)^3 \times \left(\frac{10^{33}}{1M_s}\right) = 66.7 \frac{R_e^3}{M_s s^2}, \tag{25}$$

$$m_H = 1.67 \times 10^{-24} g \times \left(\frac{M_s}{10^{33} g}\right) = 1.67 \times 10^{-57} M_s, \tag{26}$$

$$m_H = 9.11 \times 10^{-28} g \times \left(\frac{M_s}{10^{33} g}\right) = 9.11 \times 10^{-61} M_s, \tag{27}$$

$$c = 3 \times 10^{10} \frac{cm}{s} \times \left(\frac{1R_e}{10^8 cm}\right) = 300 \frac{R_e}{s}, \tag{28}$$

$$\rho_0 = \frac{n_0 m_H}{\chi_e} = \frac{5.89 \times 10^{29} \times 1.67 \times 10^{-24}}{\chi_e} \frac{g}{cm^3} \times \frac{1M_s}{10^{33} g} \times \left(\frac{10^8 cm}{R_e}\right)^3 = \frac{9.8363 \times 10^{-4}}{\chi_e} \frac{M_s}{R_e^3}. \tag{29}$$

The central densities chosen for this simulation were of the form $\kappa\rho_0$, where $\rho_0$ was defined in (9), and is the critical density demarcating non-relativistic from relativistic regimes. Values for $\kappa$ ranged from $[10^{-2}, 10^5]$. As a comparison, $\rho_0$ **roughly corresponds to the density at the centre of the sun** $(10^6 g cm^{-3})$.

# 6 Results for First Order Diff Eq

## 6.1 Mass-Radius Relationship

Figure 2 and Figure 3 show the mass-radius relationship for carbon and iron white dwarfs respectively. For lower values of central density in the non-relativistic limit, white dwarfs are less massive and larger, and the mass seems to be inversely proportional to the cube of the radius. For higher values of central density in the relativistic limit, white dwarf mass approaches the Chandrasekhar Limit and the star shrinks rapidly.

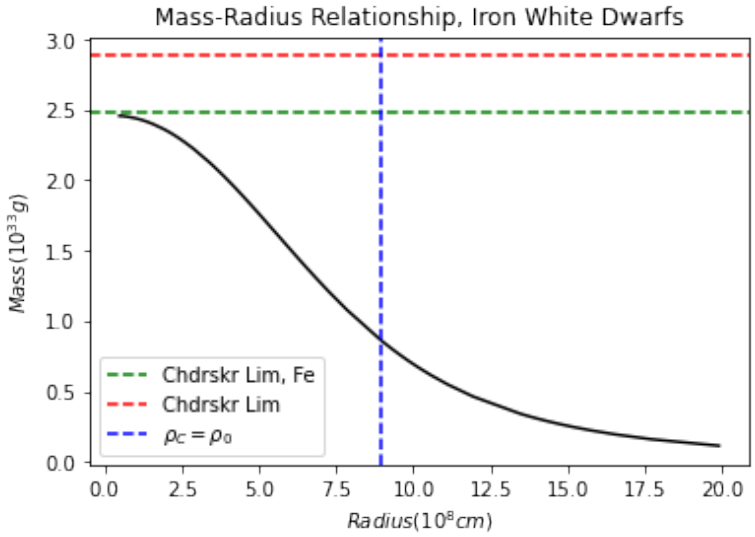


Figure 3: Mass-Radius Relationship for Iron White Dwarfs: Solutions to the stellar structure code yields the mass-radius relationship for white dwarfs, subject to a value of $chi_e$ and $\rho_C$. For iron, $\chi_e = 0.464$. The dashed vertical line demarcates non-relativistic and relativistic limits. It is seen that non-relativistic white dwarfs are less massive and larger where as relativistic white dwarfs approach a mass value, the Chandrasekhar Limit, with a rapidly shrinking radius.

### 6.2 Mass Profile and Density Profile

Figure 4 and Figure 5 show the mass profile for carbon and iron white dwarfs respectively. Each track corresponds to one star subject to a unique $\rho_C$ condition. Non-relativistic white dwarfs have an ending radius right to the dashed vertical line where as relativistic white dwarfs have an ending radius to the left of the same line.

Figure 6 and Figure 7 show the density profile for carbon and iron white dwarfs respectively. Just like the mass profile plots, each track corresponds to one star subject to a unique $\rho_C$ condition. Non-relativistic white dwarfs extend to the right of the dashed vertical line where as relativistic white dwarfs terminate left of the dashed vertical line.

### 6.3 Effect of Changing Composition

The mass-radius, mass profile, and density profile trends of carbon and iron white dwarfs are the same. The mass-radius plots are the most useful for comparing white dwarfs of different composition. Iron white dwarfs have a slightly lower Chandrasekhar mass owing to a smaller value of $\chi_e$. The Chandrasekhar mass is given by

$$M_{Ch} = 1.44 \left(\frac{\chi_e}{0.5}\right)^2 M_{sun}. \tag{30}$$

In the units adopted in this paper, $M_{Ch} = 2.88$ for carbon and $M_{Ch} \approx 2.5$ for iron. Both Figure 2 and Figure 3 confirm this with slightly different ending mass values in the relativistic tail. Analyzing the non-relativistic tail shows that that iron white dwarfs are smaller than carbon white dwarfs for the same mass.

## 7 Roy-Lane-Emden Equation: Second-Order Diff Eq

There is another method to produce the plots of Section 6 and it involves decoupling (1) and (2) and solving a second-order differential equation for density. The derivation is shown in the steps below:

$$\frac{d\rho}{dr} = \frac{-m_H}{\chi_e m_e c^2 \alpha(x)} \frac{Gm(r)\rho}{r^2} \implies \frac{\alpha(x) r^2}{\rho} \frac{d\rho}{dr} = \frac{-Gm_H}{\chi_e m_e c^2} m(r), \tag{31}$$

this re-arrangement was done to remove the mass variable upon taking the derivative with respect to radius on both sides as follows:

$$\frac{d}{dr}\left(\alpha(x) r^2 \rho^{-1} \dot{\rho}\right) = \frac{-Gm_H 4\pi r^2 \rho}{\chi_e m_e c^2}, \tag{32}$$

applying the chain rule to the left hand side we get:

$$\frac{d}{dr}\left(\alpha(x) r^2 \rho^{-1} \dot{\rho}\right) = \frac{d\alpha(x)}{dx}\frac{dx}{dr} r^2 \rho^{-1} \dot{\rho} + \alpha(x) 2r \rho^{-1} \dot{\rho} - \alpha(x) r^2 \rho^{-2} \dot{\rho}^2 + \alpha(x) r^2 \rho^{-1} \ddot{\rho}. \tag{33}$$

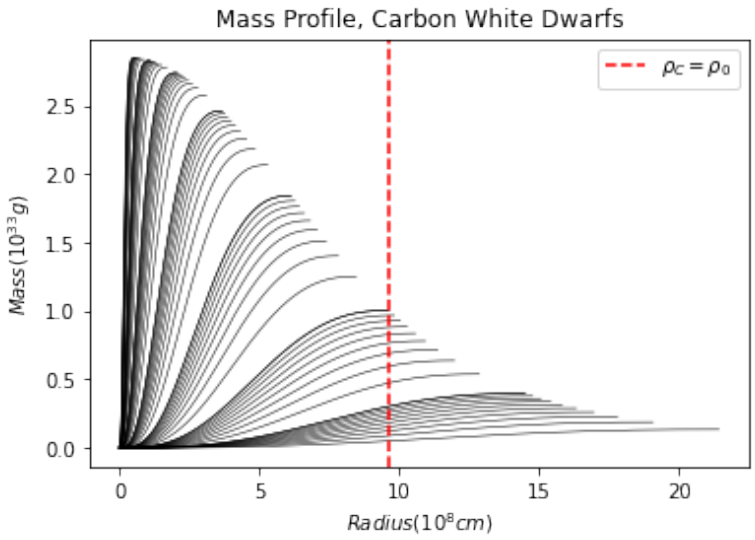


Figure 4: Mass Profile for Carbon White Dwarfs: Each track corresponds to one white dwarf's enclosed mass as a function of radius. Non-relativistic white dwarfs finish with larger radius values to the right of the dashed vertical line, where as relativistic white dwarfs finish to the left of the vertical line with smaller radii and more massive cores.

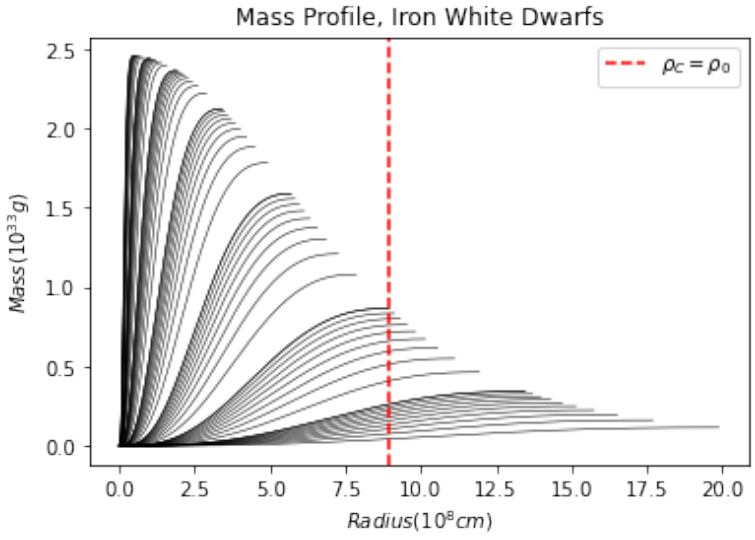


Figure 5: Mass Profile for Iron White Dwarfs: Each track corresponds to one white dwarf's enclosed mass as a function of radius. Non-relativistic white dwarfs finish with larger radius values to the right of the dashed vertical line, where as relativistic white dwarfs finish to the left of the vertical line with smaller radii and more massive cores.

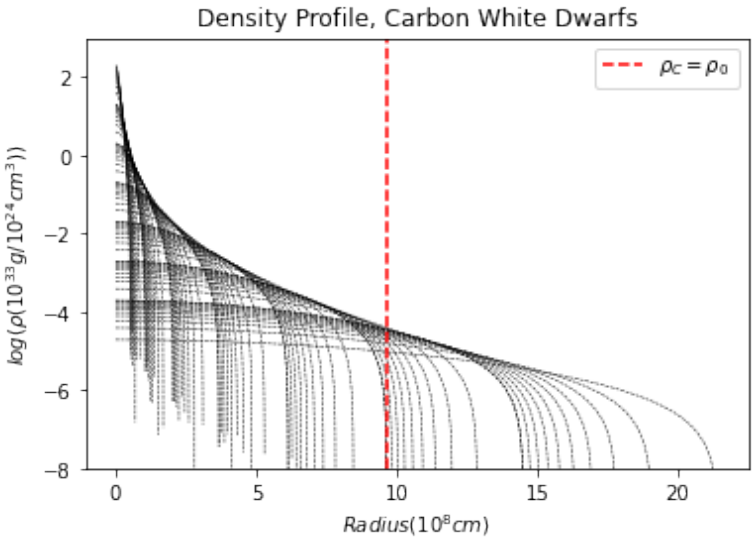


Figure 6: Density Profile for Carbon White Dwarfs: Each track corresponds to one white dwarf's density as a function of radius. Non-relativistic white dwarfs finish with larger radius values to the right of the dashed line, where as relativistic white dwarfs finish to the left of the vertical line with smaller radii and more quickly falling densities.

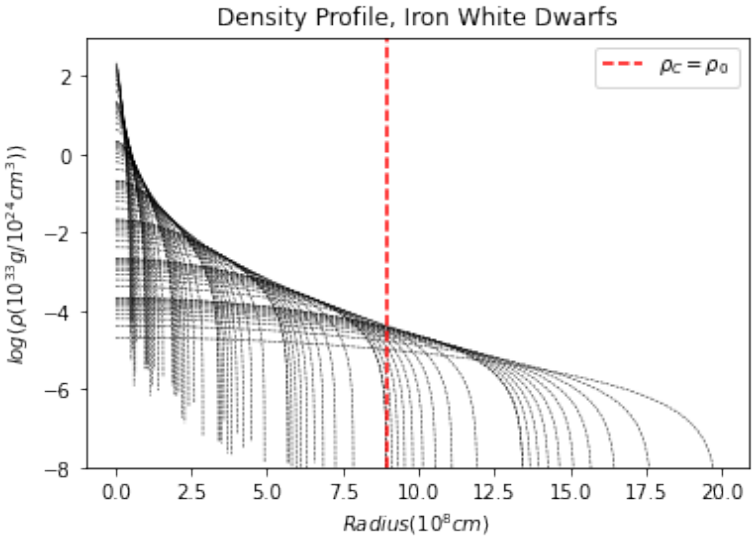


Figure 7: Density Profile for Iron White Dwarfs: Each track corresponds to one white dwarf's density as a function of radius. Non-relativistic white dwarfs finish with larger radius values to the right of the dashed line, where as relativistic white dwarfs finish to the left of the vertical line with smaller radii and more quickly falling densities.

Now isolating for $\ddot{\rho}$ which will appear in (32) after using (33) gives

$$\ddot{\rho} = \frac{-Gm_H 4\pi\rho^2}{\chi_e m_e c^2 \alpha(x)} - \left(\frac{d\alpha(x)}{dx}\frac{dx}{dr}\right)\frac{\dot{\rho}}{\alpha(x)} - \frac{2\dot{\rho}}{r} + \frac{\dot{\rho}^2}{\rho}, \tag{34}$$

where the term in parenthesis was found to be

$$\frac{d\alpha(x)}{dx}\frac{dx}{dr} = \frac{x\left(1+x^2\right)^{\frac{-1}{2}}}{3}\left(2 - x^2(1+x^2)^{-1}\right)\frac{x\dot{\rho}}{3\rho}. \tag{35}$$

The usual strategy to arrive at a second-order differential equation for $\rho$ is by the usage of the poly-tropic equation. Such a standard expression would be called the **Lane-Emden Equation**. However, since white dwarfs don't strictly obey the poly-tropic equation of state, the general equation of state was utilized. Since it is still a second-order differential equation for density of a star, I will coin (34) as the **Roy-Lane-Emden Equation for White Dwarfs**. Substituting (35) into (34), the density profile of the white dwarf was generated using the Runge-Kutta Second Order Method, the skeleton of which is given below. The results were identical to the first-order differential equation routine.

$$\dot{\rho}[i+1/2] = \dot{\rho}[i] + \ddot{\rho}[i]\frac{dr}{2}, \tag{36}$$

$$\rho[i+1/2] = \rho[i] + \dot{\rho}[i]\frac{dr}{2}, \tag{37}$$

$$\dot{\rho}[i+1] = \dot{\rho}[i] + \ddot{\rho}[i+1/2]dr, \tag{38}$$

$$\rho[i+1] = \rho[i] + \dot{\rho}[i+1/2]dr. \tag{39}$$

The vital difference between the second-order method and the first-order method is that initial values for $\rho$ and $\dot{\rho}$ are needed for the former, and not $m$ like in the latter. Also, only density is solved for in the second-order technique and if mass is required, the density values found from solving (34) can be used for a direct numeric integration as dictated by (1). The starting value for $\rho$ is the free central density parameter so $\rho(r=0) = \rho_C$, and since no mass in enclosed at $r = 0$, (2) gives $\dot{\rho}(r=0) = 0$. Now just like in the first-order case, the discontinuity at $r = 0$ prevents application of the numerical method at this point and approximations must be made. The $\dot{\rho}(r=0) = 0$ condition sets $\rho(r = dr) = \rho(r = 0) = \rho_C$. It was approximated that $\dot{\rho}(r = dr) = \dot{\rho}(r = 0) = 0$.

# 8 Conclusion

Solving for large-scale properties of a white dwarf requires usage of the physics of a minuscule and its most fundamental constituent, the electron. Uncovering the pressure-density relationship for degenerate electrons was necessary for the standard stellar structure routine, whose results matched theoretical predictions. It was observed the non-relativistic white dwarfs have smaller masses and larger radii where as relativistic white dwarfs have a limiting mass known as the Chandrasekhar Limit alongside a rapidly shrinking radius. Changing composition has little qualitative bearing on the mass-radius relationship or the mass and density profiles; precise quantitative investigation showed that iron white dwarfs are less massive in the relativistic limit and smaller in the non-relativistic limit.

# 9 Further Work

White dwarfs are the most understood out of the three eventual final fates of stars thanks to their relatively weaker gravitational density and a friendlier equation of state, but they do have some questions to answer. This paper assumed non-magnetic and non-rotating objects, a simplified model compared to a realistic white dwarf. Also, white dwarf stars in binary systems accrete mass, and these **cataclysmic variables** are waiting for a thorough mathematical treatment. Lastly, the mass-radius plot developed for white dwarfs can be tested using machine learning techniques to see how well it predicts mock data. These are all but a few ideas for further research.

# 10 Bibliography

[1] S. E. Koonin and D. C. Meredith, *COMPUTATIONAL PHYSICS: FORTRAN EDITION*, CRC Press, Taylor and Francis Group, Florida, USA, 2018.